Networks and Heterogeneous Media

NHM, 20(4): 1251–1268.
DOI: 10.3934/nhm.2025054
Received: 12 October 2025
Revised: 11 November 2025
Accepted: 18 November 2025
Published: 24 November 2025

https://www.aimspress.com/journal/NHM

Research article

Prescribed-time stabilization for nonlinear systems via hybrid continuous and dynamic event-triggered impulsive control

Yanmei Yang[1], Xiaoying Zhu[1], Lichao Feng[1,2,*] and Liping Du[1]

[1] College of Science, North China University of Science and Technology, Tangshan 063210, China
[2] Hebei Key Laboratory of Data Science and Application, North China University of Science and Technology, Tangshan 063210, China

* **Correspondence:** Email: fenglichao@ncst.edu.cn.

Abstract: Here, by integrating continuous control and dynamic event-triggered impulsive control (DETIC) based on a piecewise function ratio framework, a hybrid control strategy is developed to solve prescribed-time stabilization (PTS) for nonlinear systems. Different from the traditional methods, the designed hybrid control strategy is rooted in DETIC, and the designed triggering mechanism allows the impulsive triggering instants to be dynamically adjusted, with the Zeno behavior being eliminated. The dynamic event-triggered mechanism (DETM) is utilized to determine the instants of impulses, thereby reducing unnecessary control execution and enhancing control efficiency. Moreover, the proposed approach is utilized for the master-slave synchronization of the Lorenz system, and numerical experiments are conducted to demonstrate the practicality and efficiency of the developed hybrid control scheme.

Keywords: dynamic event-triggered impulsive control; hybrid control; prescribed-time stability; prescribed-time synchronization.

1. Introduction

Investigating the stability and developing control methods for nonlinear systems is a central topic in modern control theory and has important practical applications in engineering fields such as robot motion planning, spacecraft attitude control, and smart grid management. Traditional continuous control methods (e.g., PID control, sliding-mode control) face significant challenges in terms of the

resource efficiency, real-time performance, and robustness [1]. In addition, as a key method to handle system uncertainties and external disturbances, adaptive control combined with advanced strategies such as fuzzy logic and backstepping methods has demonstrated great potential in solving nonlinear control problems in fields of multi-agent collaboration [2], network attack protection [3], and spacecraft formation [4]. Although the above-mentioned methods have their advantages, how to achieve efficient and accurate stability control of nonlinear systems is still a difficult problem. As a type of non-continuous control method [5], impulsive control has found extensive use across various fields, including satellite orbit transfer [6], chaotic synchronization [7], and communication security [8]. So far, scholars in different fields have focused on impulsive control strategies [9]. However, traditional impulsive control mostly adopts periodic or fixed-time impulsive instants, which simplifies the controller design to a certain extent, but difficultly adapts to the dynamic changes of the system state. Fixed impulses may cause control lag or redundancy, particularly in fast-response scenarios, thus reducing the robustness of the system.

The trigger control strategy, which includes time-triggered control (TTC) and event-triggered control (ETC), is applied as a discontinuous strategy to ensure system stability and other performance. TTC usually relies on a manually set fixed sampling period [10,11], which is prone to over-sampling, resource waste, and control redundancy. In contrast, ETC only updates the controller at specific discrete instants [12–14], which are determined by the triggering conditions. At present, a variety of ETC strategies have been applied in actual control systems, such as state observation systems [15], multi-agent systems [16], and network control systems [17]. The significant advantages of ETC in resource optimization have naturally inspired its integration with impulsive control, making event-triggered impulsive control (ETIC) a key research direction [18–20]. For example, Li and Peng [18] investigated Lyapunov stability of impulsive systems under an event-triggered mechanism (ETM) and derived sufficient conditions for uniform and global asymptotic stability. Liu and Zhang [19] explored a new type of ETIC mechanism, and established the relationship between impulse intensity and ETIC. Subsequently, Li and Li [20] further expanded the robustness analysis of ETIC in terms of input-to-state stability. The aforementioned research on ETIC primarily focused on asymptotic stability or finite-time stability, with relatively limited focus on prescribed-time stabilization (PTS). PTS is a stringent control objective that requires the system to converge to an equilibrium within a prescribed-time, no matter what the initial conditions and control parameters are [21]. Compared with the existing time-bounded stability methods (e.g., finite-time and fixed-time stability) [22,23], PTS exhibits a greater application potential in scenarios demanding stringent real-time performance, such as unmanned aerial vehicle formations and high-speed robotic arms. However, many existing studies focused on the PTS design under the continuous control framework, while the analysis of PTS under discontinuous control (such as impulsive control) was still insufficient. This theoretical gap limits its application in resource-constrained but high-precision scenarios. For instance, in Unmanned Aerial Vehicle (UAV) formations, a prescribed-time convergence guarantee, under a discontinuous communication protocol, is crucial to avoid collisions and maintain the formation shape during rapid maneuvers, which requires control commands to be executed at non-periodic but precise instants. The motivation of this article is to present an enriching theoretical study on PTS under ETIC.

In the last few years, hybrid control schemes integrate the strengths of continuous and impulsive control, thus offering a new avenue to manage complex systems. For instance, [24] designed an ETIC algorithm, thereby combining the impulsive control mechanism with an ETM, thus ensuring input-to-state stability in time-delay systems. Reference [25] proposed a new type of ETM controller that integrated impulsive and sampled-data control to establish criteria for finite-time stability. Nevertheless, implementing strict PTS for nonlinear systems under the hybrid control framework, especially to

ensure the balance between the triggering frequency and the convergence accuracy, remains a challenge in current research. Addressing this challenge is crucial to deploy such controllers in practice. For example, in high-speed robotic arms, continuous control ensures smooth trajectory tracking, while impulsive control provides powerful and instantaneous corrections for sudden disturbances. A well-balanced hybrid strategy can achieve the prescribed-time positioning accuracy without overwhelming the actuator by excessive triggering. Overcoming this challenge is another motivation of this article.

In addition, a traditional ETM mostly adopt static thresholds or single time-dependent thresholds, thus making it difficult to balance the dynamic requirements of the convergence speed and steady-state accuracy. For instance, in [26], the ETM is static, that is, an event is only triggered when the measurement error reaches or exceeds a predefined threshold. To achieve a more substantial reduction in the communication overhead, the dynamic event-triggered mechanism (DETM) was proposed in [27]. In reference [28], a DETM was introduced into the design of the synchronous controller to achieve the exponential boundedness for complex dynamic networks, but this imprecise steady-state performance goal lead to fundamental limitations in its DETM design. Herein, the adopted linear DETM structure meant that its triggering strategy was in a single mode throughout the control process, and the designer must make a choice between a "faster initial convergence" and a "better steady-state accuracy" at the initial design stage and not be adjusted during operation. Li and Wu [29] investigated the problem of achieving specified-time synchronization in piecewise smooth network systems using a nonlinear DETM, where its DETM was an open-loop process with the evolution of the internal dynamic variables being designed as a fixed-driven function, that is the evolution process in [29] did not receive or respond to the feedback of real-time synchronization errors of the system, which resulted in redundant triggering. It is noteworthy that although the aforementioned studies have proposed some DETM solutions for multi-agent system synchronization, distributed control, and nonlinear system synchronization, there is still a lack of sufficient research on DETM to balance the triggering mechanism with the system performance, particularly in dynamically adjusting the trade-off between the convergence speed and steady-state accuracy. For example, take the adaptive cruise control system of unmanned vehicle fleets as follows: in the transient stage of sudden situations, the system needs to prioritize ensuring the convergence speed to achieve a rapid response; and during the steady-state stage of smooth following, it is necessary to prioritize ensuring the control accuracy and communication efficiency. For this, how to achieve the balance is an open issue. Therefore, the final motivation of this article is to understand how to design a DETM with dynamic trade-off capabilities.

Inspired by the aforementioned motivations, this paper focuses on exploring the PTS of nonlinear systems through the development of a novel DETM. Compared with prior work, this paper presents the following major contributions:

1) A DETIC method is proposed, which employs by employing the ratio of dynamic piecewise function. Specifically, this method constructs a novel time-dependent piecewise function to dynamically adjust the impulsive triggering conditions, while ensuring the avoidance of Zeno behavior and PTS of the system. Moreover, it designs a new time-dependent piecewise function.

2) A hybrid control strategy is proposed, which combines the smooth regulation of continuous control and the instantaneous intervention of impulsive control.

3) The designed hybrid control approach guarantees that the master-slave system reaches synchronization within the prescribed-time. A numerical example which involves master-slave synchronization of the chaotic Lorenz system is utilized to further validate the strategy's feasibility and practical control performance.

The remainder of the paper is structured as below: Section 2 provides essential definitions and preliminary concepts; Section 3 introduces the design of a DETM along with sufficient conditions to

achieve PTS in nonlinear systems; in Section 4, a hybrid control strategy is developed to ensure prescribed-time synchronization between the master and slave systems; Section 5 offers a simulation case to validate the effectiveness of the proposed approach ; and the conclusion is presented in Section 6.

Notations. $\|\cdot\|$ is the Euclidean norm on $\mathbb{R}^n$. $\mathbb{R}_+$, $\mathbb{Z}_+$ refer to non-negative reals and positive integers, respectively. $\mathbb{R}^{n\times m}$ represents all real matrices of size $n\times m$. I_n denotes the $n\times n$ identity matrix. $\mathcal{H}>0(\mathcal{H}<0)$ denotes a positive (negative) definite matrix. $\|\mathcal{H}\|=\sqrt{\lambda_{max}(\mathcal{H}^T\mathcal{H})}$, where $\lambda_{max}(\mathcal{H}^T\mathcal{H})$ is the maximun eigenvalue of matrix $\mathcal{H}^T\mathcal{H}$.

2. Preliminaries

Consider a general nonlinear system, $\forall \mathcal{s}\geq 0$,

$$\dot{m}(\mathcal{s})=\mathcal{f}\big(m(\mathcal{s})\big),\mathcal{s}\neq \mathcal{s}_{\mathcal{k}}, \tag{1}$$

subject to impulse

$$m(\mathcal{s})=\mathcal{g}_{\mathcal{k}}\big(m(\mathcal{s}^-)\big),\mathcal{s}=\mathcal{s}_{\mathcal{k}}, \tag{2}$$

With the initial value m_0, where $m\in\mathbb{R}^n$ represents the system state, $\dot{m}$ stands for the right-hand derivative of m, and $\mathcal{f},\mathcal{g}_{\mathcal{k}}:\mathbb{R}^n\to\mathbb{R}^n$, with $\mathcal{f}$ assumed to be locally Lipschitz. $\{\mathcal{s}_{\mathcal{k}},\mathcal{k}\in\mathbb{Z}_+\}$ is an impulsive sequence; when $\mathcal{s}\neq\mathcal{s}_{\mathcal{k}}$, the continuous evolution is determined by $\dot{m}(\mathcal{s})=\mathcal{f}\big(m(\mathcal{s})\big)$, and at the impulsive instants $\mathcal{s}=\mathcal{s}_{\mathcal{k}}$, the state is updated according to $m(\mathcal{s})=\mathcal{g}_{\mathcal{k}}\big(m(\mathcal{s}^-)\big)$. $m(\mathcal{s})$ is assumed to be right-continuous and has a left limitation (i.e., $m(\mathcal{s}_{\mathcal{k}})=m(\mathcal{s}_{\mathcal{k}}^+)$).

Definition 1. [20] Let $\mathcal{U}:\ \mathbb{R}^n\to\mathbb{R}_+$ denote a function that is locally Lipschitz continuous. Its upper-right Dini derivative along the solutions of system (1) is as follows:

$$D^+\mathcal{U}\big(m(\mathcal{s})\big)=\limsup_{\ell\to 0^+}\frac{1}{\ell}\Big[\mathcal{U}\Big(m(\mathcal{s})+\ell\mathcal{f}\big(m(\mathcal{s})\big)\Big)-\mathcal{U}\big(m(\mathcal{s})\big)\Big]. \tag{3}$$

Definition 2. [29] System (1) is globally PTS, if the following hold:

1) for every initial value $m_0\in\mathbb{R}^n$, there exists a function $0\leq T(m_0)<+\infty$ such that $\lim_{\mathcal{s}\to T(m_0)^-}m(\mathcal{s})=0$ and $m(\mathcal{s})\equiv 0$, for $\mathcal{s}\geq T(m_0)$;

2) the settling time $T(m_0)$ has an upper bound $T^*>0$, for $\forall m_0\in\mathbb{R}^n$. Here, T^* is called the prescribed-time.

The next section will introduce the following time-dependent function with a piecewise structure:

$$\mathcal{p}(\mathcal{s})=\begin{cases}\alpha ln(1+T^*-\mathcal{s}),\mathcal{s}\in[0,T^*)\\ e^{-\theta\mathcal{s}},\mathcal{s}\in[T^*,+\infty)\end{cases}, \tag{4}$$

where $\alpha>0$ and $\theta>0$ are adjustable constants. Then,

$$\dot{\mathcal{p}}(\mathcal{s})=\begin{cases}\frac{-\alpha}{1+T^*-\mathcal{s}},\mathcal{s}\in[0,T^*)\\ -\theta e^{-\theta\mathcal{s}},\mathcal{s}\in[T^*,+\infty)\end{cases}. \tag{5}$$

When $\mathcal{s}\in[0,T^*)$, $\mathcal{p}(\mathcal{s})$ is strictly monotonically decreasing, $\mathcal{p}(0)=\alpha ln(1+T^*)$, and $\lim_{\mathcal{s}\to T^*}\mathcal{p}(\mathcal{s})=0$; and when $\mathcal{s}\in[T^*,+\infty)$, $\lim_{\mathcal{s}\to+\infty}\mathcal{p}(\mathcal{s})=0$.

In essence, this function effectively describes the time-dependent dynamics of the system by adopting different expressions on $[0,T^*)$ and $[T^*,+\infty)$. Specifically, $\wp(\mathcal{s})$ is strictly monotonically decreasing on $[0,T^*)$ and tends to zero at $\mathcal{s}=T^*$; alternatively, on $[T^*,+\infty)$, $\wp(\mathcal{s})$ gradually approaches zero.

3. Event-triggered mechanism

Here, we aim to adopt a control strategy based on a DETM to adaptively adjust the impulsive triggering instants and eliminate the Zeno behavior. Specifically, the DETM is designed as follows:

$$\mathcal{s}_{\mathcal{k}}=inf\left\{\mathcal{s}\geq\mathcal{s}_{\mathcal{k}-1},\mathcal{U}\big(m(\mathcal{s})\big)\geq\frac{\wp(\mathcal{s})}{\wp(\mathcal{s}_{\mathcal{k}-1})}\mathcal{U}\big(m(\mathcal{s}_{\mathcal{k}-1})\big)\right\},\tag{6}$$

where the function $\mathcal{U}\big(m(\mathcal{s})\big)$ represents the Lyapunov function of system (1) when $\mathcal{s}_0=0$.

The DETM (6) implies that triggering instants $\{\mathcal{s}_{\mathcal{k}},\mathcal{k}\in\mathbb{Z}_+\}$ are determined by the ratio of $\wp(\mathcal{s})$ and may vary with the choice of $\mathcal{U}\big(m(\mathcal{s})\big)$. Among them, the piecewise function $\wp(\mathcal{s})$ is monotonically decreasing in each time period, thus causing the threshold of impulsive triggering to gradually decrease over time. It should be particularly emphasized that the threshold is relatively high and the triggering frequency is low in the early stage, thus avoiding excessive control; in the later stage, as $\wp(\mathcal{s})$ decreases, the triggering threshold also accordingly decreases to ensure that the system gradually converges to the desired state. Additionally, the threshold can be modified in response to changes in the system's dynamics, thereby avoiding unnecessary activation and improving the overall efficiency and responsiveness of the system.

Remark 1. The existing research on the ETM (e.g. [18]) mostly adopts static thresholds or single attenuation functions (e.g. exponential thresholds), and its limitation lies in the inability to dynamically adapt to the phased requirements of the system state. This study proposes a dynamic ratio triggering condition. The triggering threshold dynamically decays with $\wp(\mathcal{s})\,/\,\wp(\mathcal{s}_{\mathcal{k}-1})$, which not only reflects the convergence requirement at the current instant but also inherits the state information of the previous triggering instant, thus avoiding false triggering caused by instantaneous disturbances.

Theorem 1: Suppose that $\mathcal{U}:\mathbb{R}^n\to\mathbb{R}_+$ is a locally Lipschitz continuous function which satisfies $\mathcal{U}(0)\equiv 0$. Given the prescribed-time $T^*>0$, assume there exist constants $\tau>0$, $a_{\mathcal{k}}>0$, and a bounded, time-dependent function $c(\mathcal{s})$ that is negative for all $\mathcal{s}$, such that

$$D^+\mathcal{U}\big(m(\mathcal{s})\big)\leq\tau c(\mathcal{s})\mathcal{U}\big(m(\mathcal{s})\big),\mathcal{s}\neq\mathcal{s}_{\mathcal{k}},\tag{7}$$

$$\mathcal{U}\left(g_{\mathcal{k}}\big(m(\mathcal{s})\big)\right)\leq e^{-a_{\mathcal{k}}}\mathcal{U}\big(m(\mathcal{s})\big),\mathcal{s}=\mathcal{s}_{\mathcal{k}},\tag{8}$$

where $\{\mathcal{s}_{\mathcal{k}},\mathcal{k}\in\mathbb{Z}_+\}$ is generated by the DETM (6); then system (1) is globally PTS.

Proof. Let $m(\mathcal{s})$ represent the solution of system (1). Evidently, if the event is triggered finitely or not at all on $[\mathcal{s}_0,+\infty)$, then the Zeno behavior can be directly avoided. Consequently, we focus on the case of infinite event triggering. From Eq (6), the sequence $\{\mathcal{s}_{\mathcal{k}}\}$ satisfies $\mathcal{s}_0\leq\mathcal{s}_1\leq\mathcal{s}_2\leq\cdots\leq\mathcal{s}_{\mathcal{k}}\leq\cdots$; then, we prove that no Zeno behavior occurs.

From Eq (7), there exists a positive constant ϵ that satisfies $0<\epsilon<\tau$ such that Eq (9) holds:

$$\begin{aligned}D^+\mathcal{U}\big(m(\mathcal{s})\big)&\leq\tau c(\mathcal{s})\mathcal{U}\big(m(\mathcal{s})\big)\\&<(\tau-\epsilon)c(\mathcal{s})\mathcal{U}\big(m(\mathcal{s})\big).\end{aligned}\tag{9}$$

From Eq (9), one has the following:

$$\mathcal{U}\big(m(\mathcal{s}_1)\big) < e^{(\tau-\epsilon)\int_{\mathcal{s}_0}^{\mathcal{s}_1} c(\mathcal{s})\,d\mathcal{s}}\mathcal{U}\big(m(\mathcal{s}_0)\big).$$

Then, from Eq (6) for $\mathcal{s} \in [\mathcal{s}_0,\mathcal{s}_1)$,

$$\begin{aligned}\mathcal{U}\big(m(\mathcal{s}_1)\big) &= \frac{\mathcal{p}(\mathcal{s}_1)}{\mathcal{p}(\mathcal{s}_0)}\mathcal{U}\big(m(\mathcal{s}_0)\big)\\ &< e^{(\tau-\epsilon)\int_{\mathcal{s}_0}^{\mathcal{s}_1} c(\mathcal{s})\,d\mathcal{s}}\mathcal{U}\big(m(\mathcal{s}_0)\big).\end{aligned} \tag{10}$$

Since $c(\mathcal{s}) < 0$, then $e^{(\tau-\epsilon)\int_{\mathcal{s}_0}^{\mathcal{s}_1} c(\mathcal{s})\,d\mathcal{s}} \leq 1$, and $\frac{\mathcal{p}(\mathcal{s}_1)}{\mathcal{p}(\mathcal{s}_0)} < 1$. Since $\mathcal{p}(\mathcal{s})$ is strictly monotonically decreasing, $\mathcal{p}(\mathcal{s}_1) < \mathcal{p}(\mathcal{s}_0)$, which implies that $\mathcal{s}_1 > \mathcal{s}_0$.

Similarly, for $\mathcal{s} \in [\mathcal{s}_1,\mathcal{s}_2)$, we can obtain the following:

$$\mathcal{U}\big(m(\mathcal{s}_2)\big) \leq e^{\tau\int_{\mathcal{s}_1}^{\mathcal{s}_2} c(\mathcal{s})\,d\mathcal{s}}\mathcal{U}\big(m(\mathcal{s}_1)\big) < e^{(\tau-\epsilon)\int_{\mathcal{s}_1}^{\mathcal{s}_2} c(\mathcal{s})\,d\mathcal{s}}\mathcal{U}\big(m(\mathcal{s}_1)\big). \tag{11}$$

From Eq (6), we have the following:

$$\mathcal{U}\big(m(\mathcal{s}_2)\big) = \frac{\mathcal{p}(\mathcal{s}_2)}{\mathcal{p}(\mathcal{s}_1)}\mathcal{U}\big(m(\mathcal{s}_1)\big) < e^{(\tau-\epsilon)\int_{\mathcal{s}_1}^{\mathcal{s}_2} c(\mathcal{s})\,d\mathcal{s}}\mathcal{U}\big(m(\mathcal{s}_1)\big). \tag{12}$$

For $\int_{\mathcal{s}_1}^{\mathcal{s}_2} c(\mathcal{s})\,d\mathcal{s} < 0$, it follows that $e^{\tau\int_{\mathcal{s}_1}^{\mathcal{s}_2} c(\mathcal{s})\,d\mathcal{s}} \leq 1$. Consequently, $\frac{\mathcal{p}(\mathcal{s}_2)}{\mathcal{p}(\mathcal{s}_1)} < 1$. Since $\mathcal{p}(\mathcal{s})$ is strictly monotonically decreasing, it follows that $\mathcal{s}_2 > \mathcal{s}_1$. Through mathematical induction, it is evident that $\mathcal{s}_\varrho - \mathcal{s}_{\varrho-1} > 0$ holds for all $\varrho \in \mathbb{Z}_+$, thereby excluding the Zeno behavior.

Then, we will prove the PTS of system (1) under the DETM (6). Since the Zeno behavior has been excluded, the triggering number of a finite interval is finite. Let $\mathcal{s}_N$ denote the last triggering instant on $[\mathcal{s}_0,T^*)$.

Step 1. Consider $\mathcal{s} \in [\mathcal{s}_0,T^*)$. From the DETM (6),

$$\mathcal{U}\big(m(\mathcal{s}_1)\big) = \frac{\mathcal{p}(\mathcal{s}_1)}{\mathcal{p}(\mathcal{s}_0)}\mathcal{U}\big(m(\mathcal{s}_0)\big). \tag{13}$$

For $\forall \mathcal{s} \in [\mathcal{s}_0,\mathcal{s}_1)$, from Eq (6), we obtain the following:

$$\mathcal{U}\big(m(\mathcal{s})\big) \leq \frac{\mathcal{p}(\mathcal{s})}{\mathcal{p}(\mathcal{s}_0)}\mathcal{U}\big(m(\mathcal{s}_0)\big). \tag{14}$$

Thus,

$$\mathcal{U}\big(m(\mathcal{s}_1^-)\big) \leq \frac{\mathcal{p}(\mathcal{s}_1)}{\mathcal{p}(\mathcal{s}_0)}\mathcal{U}\big(m(\mathcal{s}_0)\big). \tag{15}$$

At the event-triggering instant $\mathcal{s}_2$, we have the following:

$$\mathcal{U}\big(m(\mathcal{s}_2)\big) = \frac{\mathcal{p}(\mathcal{s}_2)}{\mathcal{p}(\mathcal{s}_1)}\mathcal{U}\big(m(\mathcal{s}_1)\big). \tag{16}$$

For $\forall \mathcal{s} \in [\mathcal{s}_1,\mathcal{s}_2)$, the DETM (6) implies the following:

$$\mathcal{U}\big(m(s)\big) \le \frac{p(s)}{p(s_1)}\mathcal{U}\big(m(s_1)\big). \tag{17}$$

Thus,

$$\mathcal{U}\big(m(s_2^-)\big) \le \frac{p(s_2)}{p(s_1)}\mathcal{U}\big(m(s_1)\big). \tag{18}$$

By Eq (8), we have $\mathcal{U}\Big(g_1\big(m(s_1)\big)\Big) \le e^{-a_1}\mathcal{U}\big(m(s_1)\big)$, and from Eqs (15) and (18),

$$\begin{aligned}\mathcal{U}\big(m(s)\big) &\le \frac{p(s)}{p(s_1)}\mathcal{U}\Big(g_1\big(m(s_1^-)\big)\Big)\\ &\le e^{-a_1}\frac{p(s)}{p(s_1)}\mathcal{U}\big(m(s_1^-)\big)\\ &\le e^{-a_1}\frac{p(s)}{p(s_1)}\frac{p(s_1)}{p(s_0)}\mathcal{U}\big(m(s_0)\big)\\ &\le e^{-a_1}\frac{p(s)}{p(s_0)}\mathcal{U}\big(m(s_0)\big).\end{aligned} \tag{19}$$

Similarly, for $\forall s \in [s_2,s_3)$,

$$\begin{aligned}\mathcal{U}\big(m(s)\big) &\le \frac{p(s)}{p(s_2)}\mathcal{U}\Big(g_2\big(m(s_2^-)\big)\Big)\\ &\le e^{-a_2}\frac{p(s)}{p(s_2)}\mathcal{U}\big(m(s_2^-)\big)\\ &\le e^{-a_2}\frac{p(s)}{p(s_2)}\frac{p(s_2)}{p(s_1)}\mathcal{U}\big(m(s_1)\big)\\ &= e^{-a_2}\frac{p(s)}{p(s_2)}\frac{p(s_2)}{p(s_1)}\mathcal{U}\Big(g_1\big(m(s_1^-)\big)\Big)\\ &\le e^{-a_2}e^{-a_1}\frac{p(s)}{p(s_2)}\frac{p(s_2)}{p(s_1)}\mathcal{U}\big(m(s_1^-)\big)\\ &\le e^{-a_2-a_1}\frac{p(s)}{p(s_0)}\mathcal{U}\big(m(s_0)\big).\end{aligned} \tag{20}$$

For $\forall s \in [s_{N-1},s_N)$, it follows from the DETM (6) that $\mathcal{U}\big(m(s_N^-)\big) \le \frac{p(s_N)}{p(s_{N-1})}\mathcal{U}\big(m(s_{N-1})\big)$. By analogy, for $\forall s \in [s_N,T^*)$,

$$\begin{aligned}\mathcal{U}\big(m(s)\big) &\le \frac{p(s)}{p(s_N)}\mathcal{U}\big(m(s_N)\big)\\ &\le \frac{p(s)}{p(s_N)}\mathcal{U}\Big(g_N\big(m(s_N^-)\big)\Big)\\ &\le e^{-a_N}\frac{p(s)}{p(s_N)}\mathcal{U}\big(m(s_N^-)\big)\\ &\le e^{-a_N}\frac{p(s)}{p(s_N)}\frac{p(s_N)}{p(s_{N-1})}\mathcal{U}\big(m(s_{N-1})\big)\\ &= e^{-a_N}\frac{p(s)}{p(s_N)}\frac{p(s_N)}{p(s_{N-1})}\mathcal{U}\Big(g_{N-1}\big(m(s_{N-1}^-)\big)\Big)\\ &\le e^{-a_N}e^{-a_{N-1}}\frac{p(s)}{p(s_N)}\frac{p(s_N)}{p(s_{N-1})}\mathcal{U}\big(m(s_{N-1}^-)\big)\end{aligned}$$

$$
\begin{aligned}
&\leq e^{-a_N} e^{-a_{N-1}} \frac{p(s)}{p(s_N)} \frac{p(s_N)}{p(s_{N-1})} \frac{p(s_{N-1})}{p(s_{N-2})} \mathcal{U}\big(m(s_{N-2})\big) \\
&= e^{-a_N} e^{-a_{N-1}} \frac{p(s)}{p(s_N)} \frac{p(s_N)}{p(s_{N-1})} \frac{p(s_{N-1})}{p(s_{N-2})} \mathcal{U}\left(g_{N-2}\big(m(s_{N-2}^-)\big)\right) \\
&\leq e^{-a_N} e^{-a_{N-1}} e^{-a_{N-2}} \frac{p(s)}{p(s_N)} \frac{p(s_N)}{p(s_{N-1})} \frac{p(s_{N-1})}{p(s_{N-2})} \mathcal{U}\big(m(s_{N-2}^-)\big) \\
&\leq \cdots \\
&\leq e^{-(a_N + a_{N-1} + \cdots + a_1)} \frac{p(s)}{p(s_N)} \frac{p(s_N)}{p(s_{N-1})} \frac{p(s_{N-1})}{p(s_{N-2})} \cdots \frac{p(s_1)}{p(s_0)} \mathcal{U}\big(m(s_0)\big) \\
&\leq e^{-(a_N + a_{N-1} + \cdots + a_1)} \frac{p(s_1)}{p(s_0)} \mathcal{U}\big(m(s_0)\big),
\end{aligned}
\tag{21}
$$

which implies that

$$
\begin{aligned}
\mathcal{U}\big(m(s)\big) &\leq e^{-(a_N + a_{N-1} + \cdots + a_1)} \frac{p(s)}{p(s_0)} \mathcal{U}\big(m(s_0)\big) \\
&= e^{-(a_N + a_{N-1} + \cdots + a_1)} \frac{\alpha \ln(1 + T^* - s)}{\alpha \ln(1 + T^*)} \mathcal{U}\big(m(s_0)\big).
\end{aligned}
\tag{22}
$$

Since the Zeno behavior has been excluded on $[s_0, T^*)$, the triggering number N within any finite time interval must be finite (i.e., $N < +\infty$). For a_i being a positive constant, the finiteness of N directly implies $\sum_{i=1}^{N} a_i < +\infty$. It guarantees that the term $e^{-(a_N + a_{N-1} + \cdots + a_1)}$ in the stability analysis remains strictly positive and does not tend to zero as $s \to T^*$. Based on the continuity and the monotonically decreasing property of $\mathcal{U}\big(m(s)\big)$, it can be derived that $0 \leq \mathcal{U}\big(m(T^*)\big) \leq \lim_{s \to T^{*-}} \mathcal{U}\big(m(s)\big) = 0$. Therefore, $\lim_{s \to T^*} \mathcal{U}\big(m(s)\big) = 0$ and $\lim_{s \to T^*} m(s) = 0$.

Step 2. Consider $s \in [T^*, +\infty)$. From Eq (7), (8) and the monotonically decreasing property of $\mathcal{U}\big(m(s)\big)$, it follows that $m(s) \equiv 0$ for all $s > T^*$.

Consequently, by combining the above two steps, system (1) attains global PTS within the T^*. This completes the proof.

Remark 2. T^* is user-defined and preselected based on practical requirements, independent of the system parameters and initial conditions. Unlike [30], which mainly focused on pre-fixed or periodically designed impulsive triggering instants, this paper proposes a DETIC mechanism, and our method enables the impulsive triggering instants to be dynamically adjusted, thus providing greater flexibility.

Remark 3. $c(s)$ is a negative bounded time-dependent function, that is, $c(s)$ has a lower bound as $s \to T^*$. Unlike [30], whose Lyapunov derivative tends to $-\infty$ as $s \to T^*$, this paper avoids the singularity issue of unbounded control gains near T^*. In particular, $c(s)$ ensures the monotonic decreasing property of $\mathcal{U}\big(m(s)\big)$ and plays a role in eliminating the Zeno behavior, thus enabling the system to be stable within the prescribed-time while maintaining good engineering feasibility. Therefore, the condition adopted here achieves a balance between the convergence rate and the practical stability.

Remark 4. Unlike a fixed-threshold ETM, our DETM avoids premature triggering or lagging caused by static thresholds. Compared to the exponential decay trigger in [18–20], our proposed piecewise function $p(s)$ is two-stage time-dependent. It accelerates the convergence rate in a prescribed-time, and improves the performance of the traditional method which relies on a single attenuation mode and lacks dynamics.

4. Synchronization in master-slave frameworks

The following analysis applies the proposed ETIC strategy to achieve prescribed-time synchronization for master-slave systems as follows:

$$\begin{cases}(\mathcal{M})\dot{m}(s) = \mathcal{H}m(s) - g\big(m(s)\big)\\ (S)\dot{z}(s) = \mathcal{H}z(s) - g\big(z(s)\big) + v(s)\end{cases}, \tag{23}$$

where the master system is $m(s) \in \mathbb{R}^n$, and the slave system is $z(s) \in \mathbb{R}^n$. The hybrid control input is described by $v(s)$. To analyze synchronization, define the error as $w(s) = z(s) - m(s)$, and its dynamic behavior evolves as follows:

$$\begin{aligned}\dot{w}(s) &= \dot{z}(s) - \dot{m}(s)\\ &= \mathcal{H}\big(z(s) - m(s)\big) - \Big(g\big(z(s)\big) - g\big(m(s)\big)\Big) + v(s)\\ &= \mathcal{H}w(s) - \mathcal{G}\big(w(s)\big) + v(s),\end{aligned} \tag{24}$$

where $\mathcal{G}\big(w(s)\big) = g\big(z(s)\big) - g\big(m(s)\big)$.

Definition 5. [31,32] Given $T^* > 0$, the global prescribed-time synchronization of system (23) is achieved under the designed controller $v(s)$ if

$$\begin{cases}\lim\limits_{s\to T^*} w(s) = 0, s \in [0, T^*),\\ w(s) \equiv 0, s \in [T^*, +\infty).\end{cases} \tag{25}$$

Assumption 1. Function $g: \mathbb{R}^n \to \mathbb{R}^n$ is QUAD(Δ,$\mho$), i.e., there exist $n \times n$ diagonal matrices Δ and a scalar $\mho > 0$ such that, for any $m, z \in \mathbb{R}^n$,

$$(z - m)^T\big(g(z) - g(m)\big) \le (z - m)^T(\Delta - \mho I_n)(z - m).$$

Similarly to Eq (6), design the following DETM:

$$s_k = inf\left\{s \ge s_{k-1}, \mathcal{U}\big(w(s)\big) \ge \frac{p(s)}{p(s_{k-1})}\mathcal{U}\big(w(s_{k-1})\big)\right\}, \tag{26}$$

and the hybrid control is as follows:

$$v(s) = \begin{cases}v_1(s) = -Kw(s) + \beta c(s)w(s), s \ne s_k,\\ v_2(s) = Dw(s)\delta(s - s_k), \qquad s = s_k.\end{cases} \tag{27}$$

Here, $\beta > 0$, $K \in \mathbb{R}^{n\times n}$ is a gain matrix, and $D \in \mathbb{R}^{n\times n}$ is an impulsive gain matrix which satisfies $\lambda_{max}\{[(I + D)^{-1}]^T(I + D)^{-1}\} \le e^{-a_k}$, and the Dirac impulsive $\delta(s - s_k)$ introduces an instantaneous impulsive effect at $s = s_k$ and causes a discontinuous jump. Let $w(s_k^-)$ denote the pre-jump state immediately before $s = s_k$, and $w(s_k^+)$ denote the post-jump state immediately after $s = s_k$. To characterize the state jump, we integrate both sides of Eq (24) over $[s_k^-, s_k^+]$ and obtain the following:

$$\int_{s_k^-}^{s_k^+} \dot{w}(s)\, ds = \int_{s_k^-}^{s_k^+} \Big(\mathcal{H}w(s) - \mathcal{G}\big(w(s)\big) + Dw(s)\delta(s - s_k)\Big)\, ds. \tag{28}$$

Since $\mathcal{H}w(s)$ and $\mathcal{G}(w(s))$ are continuous at s_k, their instantaneous change at s_k is zero. For $Dw(s)\delta(s-s_k)$, by the property of the Dirac delta impulsive, $\int_{s_k^-}^{s_k^+} Dw(s)\delta(s-s_k)\,ds = Dw(s_k)$. Then, Eq (24) is rewritten in the following form:

$$\begin{cases} \dot{w}(s) = \mathcal{H}w(s) - \mathcal{G}(w(s)) + v_1(s), & s \neq s_k, \\ w(s_k^-) = (I-D)w(s_k), & s = s_k. \end{cases} \tag{29}$$

Theorem 2. Given that Assumption 1 holds, if there exist constants $a_k > 0$, matrices $\mathcal{H}$, and K such that $\lambda_{max}\{[(I-D)^{-1}]^T(I-D)^{-1}\} \leq e^{-a_k}$ and $\lambda_{max}(\mathcal{H} - (\Delta - \mho I_n) - K) \leq 0$ hold, then the error system (29) is globally PTS under the DETM (26) and controller (27).

Proof. Consider $\mathcal{U}(w(s)) = \frac{1}{2}w^T(s)w(s)$ and its following derivative:

$$\dot{\mathcal{U}}(w(s)) = w^T(s)\dot{w}(s). \tag{30}$$

Next, we consider two scenarios: $s \neq s_k$ and $s = s_k$.

Case 1: $s \neq s_k$**.** Substituting $v_1(s)$ into Eq (29) yields the following:

$$\dot{w}(s) = \mathcal{H}w(s) - \mathcal{G}(w(s)) - Kw(s) + \beta c(s)w(s), \tag{31}$$

Then, from Eq (30) and Assumption 1,

$$\begin{aligned} \dot{\mathcal{U}}(w(s)) &= w^T(s)\big[\mathcal{H}w(s) - \mathcal{G}(w(s)) - Kw(s) + \beta c(s)w(s)\big] \\ &= w^T(s)\mathcal{H}w(s) - w^T(s)\mathcal{G}(w(s)) - w^T(s)Kw(s) + \beta c(s)w^T(s)w(s) \\ &\leq w^T(s)\mathcal{H}w(s) - w^T(t)(\Delta - \mho I_n)w(s) - w^T(s)Kw(s) \\ &\quad +\beta c(s)w^T(s)w(s) \\ &= w^T(s)(\mathcal{H} - (\Delta - \mho I_n) - K)w(s) + \beta c(s)w^T(s)w(s) \\ &\leq \lambda_{max}(\mathcal{H} - (\Delta - \mho I_n) - K) \parallel w(s) \parallel^2 + \beta c(s) \parallel w(s) \parallel^2 \\ &\leq \beta c(s) \parallel w(s) \parallel^2 \\ &= \tau c(s)\mathcal{U}(w(s)). \end{aligned} \tag{32}$$

Here, $\tau = 2\beta$.

Case 2: $s = s_k$. From Eq (29),

$$\begin{aligned} \mathcal{U}(w(s_k)) &= \frac{1}{2}w^T(s_k)w(s_k) \\ &= \frac{1}{2}w^T(s_k^-)[(I-D)^{-1}]^T(I-D)^{-1}w(s_k^-) \\ &\leq e^{-a_k}\mathcal{U}\big(\omega(s_k^-)\big). \end{aligned} \tag{33}$$

According to the above two cases, Theorem 1 is satisfied. Then, by the DETM (26) and Theorem 1, the error system (29) is globally PTS.

Remark 5. Theorem 2 indicates that system (23) achieves global prescribed-time synchronization under a user-defined settling time T^*. Moreover, Theorem 2 can be regarded as an application of Theorem 1.

Remark 6. In essence, the triggering mechanism (26) directly adopts the triggering logic of Theorem 1. Condition $\lambda_{max}(\mathcal{H}-(\Delta-\mho I_n)-K)\leq 0$ in Theorem 2 essentially embeds condition (7) of Theorem 1 into the master-slave system (23). The QUAD assumption on $\mathcal{G}(w(s))$ and the design of continuous control gain K are to ensure that the error energy monotonically decreases on impulsive intervals. Furthermore, the nonlinear characteristics of the master-slave system (23) further test the robustness of our DETM, indicating that Theorem 1 can adapt to complex dynamic environments.

Remark 7. Different from the hybrid ETM based on state threshold which switched to either continuous control or impulsive control in [25], the DETM proposed here is specifically designed for impulsive control triggering, while the continuous control operates independently on impulsive intervals. This design decouples the triggering logic of continuous and impulsive control, thus eliminating the computational burden of real-time switching decisions. It ensures a rapid response for large deviations via impulsive control and maintains continuous suppression for minor disturbances.

5. An example

A simulation example of the chaotic Lorenz system confirms the validity of the proposed scheme. Consider the following master-slave chaotic Lorentz system:

$$\begin{cases}(\mathcal{M})\dot{m}(s)=\mathcal{H}m(s)-g\big(m(s)\big)\\(S)\dot{z}(s)=\mathcal{H}z(s)-g\big(z(s)\big)+v(s)\end{cases}, \tag{34}$$

where $m(s),z(s)\in\mathbb{R}^3$, $g\big(m(s)\big)=[0,-m_1(s)m_3(s),m_1(s)m_2(s)]^T$, $g\big(z(s)\big)=[0,-z_1(s)z_3(s),z_1(s)z_2(s)]^{\mathrm{T}}$, and $\mathcal{H}=\begin{pmatrix}-10 & 10 & 0\\ 28 & -1 & 0\\ 0 & 0 & -\frac{8}{3}\end{pmatrix}$. Assumption 1 holds for $\Delta-\mho I_3=\begin{pmatrix}31.8 & 0 & 0\\ 0 & 35 & 0\\ 0 & 0 & 32.5\end{pmatrix}$. Assume $m(0)=[-10,12,6]^T$ and $z(0)=[6,-1,16]^T$; then, for the error system (24), $w(0)=[16,-13,10]^T$.

From computer simulations (Figures 1 and 2), system (34) is not prescribed-time synchronous with $T^*=2$. To achieve prescribed-time synchronization for system (34), we set the parameters as $\alpha=3$ and $\theta=2$ for $p(s)$, and the import controller (27) with $c(s)=-0.1se^{-0.1s}$, $K=\begin{pmatrix}3 & 0 & 0\\ 0 & 3 & 0\\ 0 & 0 & 3\end{pmatrix}$, $\beta=1.5$, and $\mathrm{D}=\begin{pmatrix}0.6 & 0 & 0\\ 0 & 0.6 & 0\\ 0 & 0 & 0.6\end{pmatrix}$.

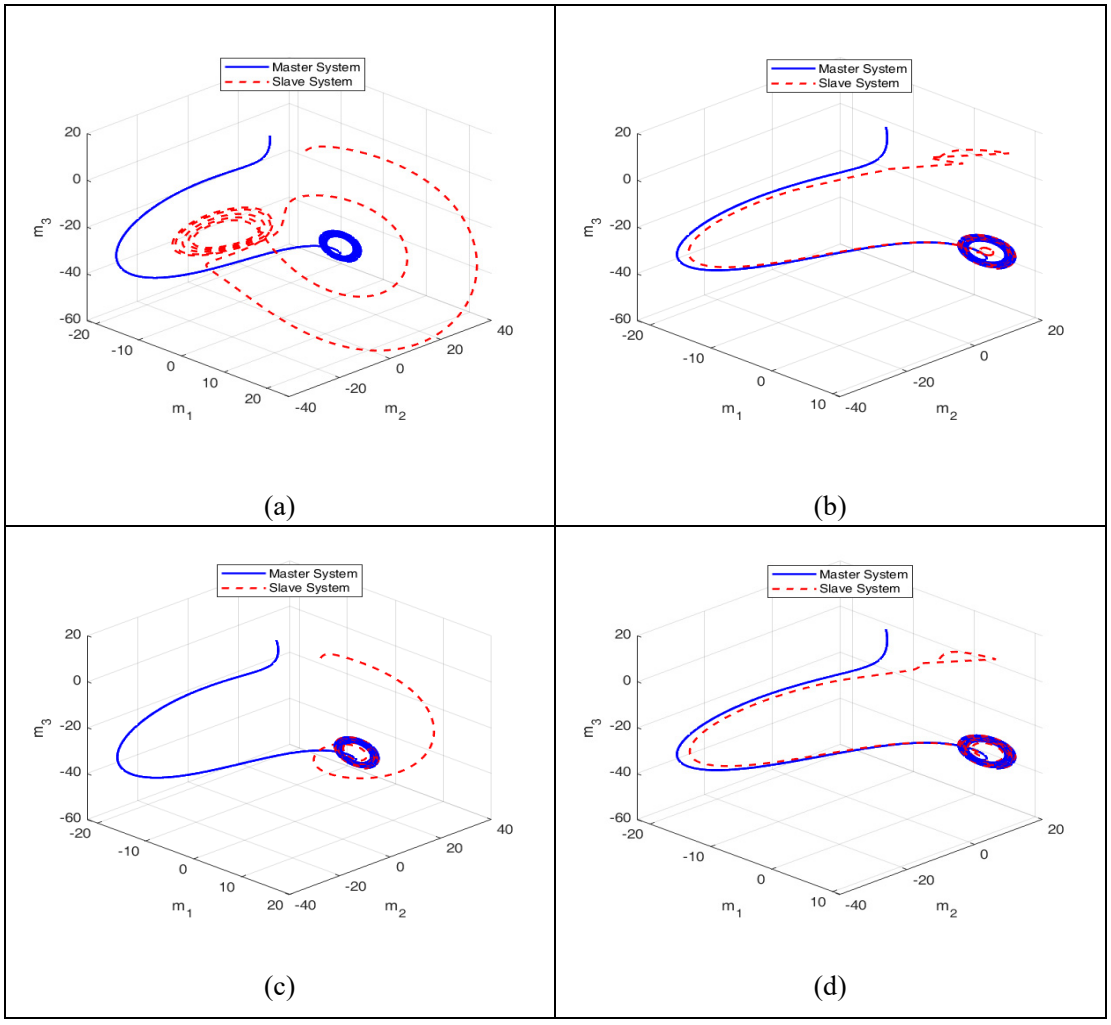

Figure 1. 3D phase space trajectories of system (34): (a) No control; (b) DETIC only; (c) Continuous control only; (d) Hybrid control.

Figure 1(a)–(d) depict the 3D chaotic phase diagrams of system (34) with no control, only DETIC, only continuous control, and hybrid control, respectively. Specifically speaking, only continuous control refers to solely having $\upsilon_1(s)$ be imported for system (34). Only DETIC control means that only the discrete control term $\upsilon_2(s)$ based on the DETM (26) is imported for system (34). Hybrid control means that $\upsilon(s)$ based on both continuous control and DETIC is imported for system (34).

Figure 2(a)–(d) depict the 2D trajectories of system (34). Figure 2(b) shows that under the DETM (26), the control signal only acts at 23 specific triggering instants on [0,5] marked with asterisks. Figure 2(c) shows that when only $\upsilon_1(t)$ is available, the trajectory can be effectively smoothed, thus significantly reducing oscillations and gradually stabilizing the system. The hybrid control in Figure 2(d) combines the advantages of continuous control and DETIC. The system is continuously adjusted under smooth control $\upsilon_1(t)$, while the impulsive control is applied for intervention at triggering instants. Remarkably, the hybrid control strategy reduces the triggering frequency by 47.8% (from 23 triggering numbers to 12 ones) compared to only DETIC; as shown in Figure 3, in comparison with the scenario using only DETIC, the hybrid control significantly reduces the number triggering, thus optimizing the responsiveness and stability of the system.

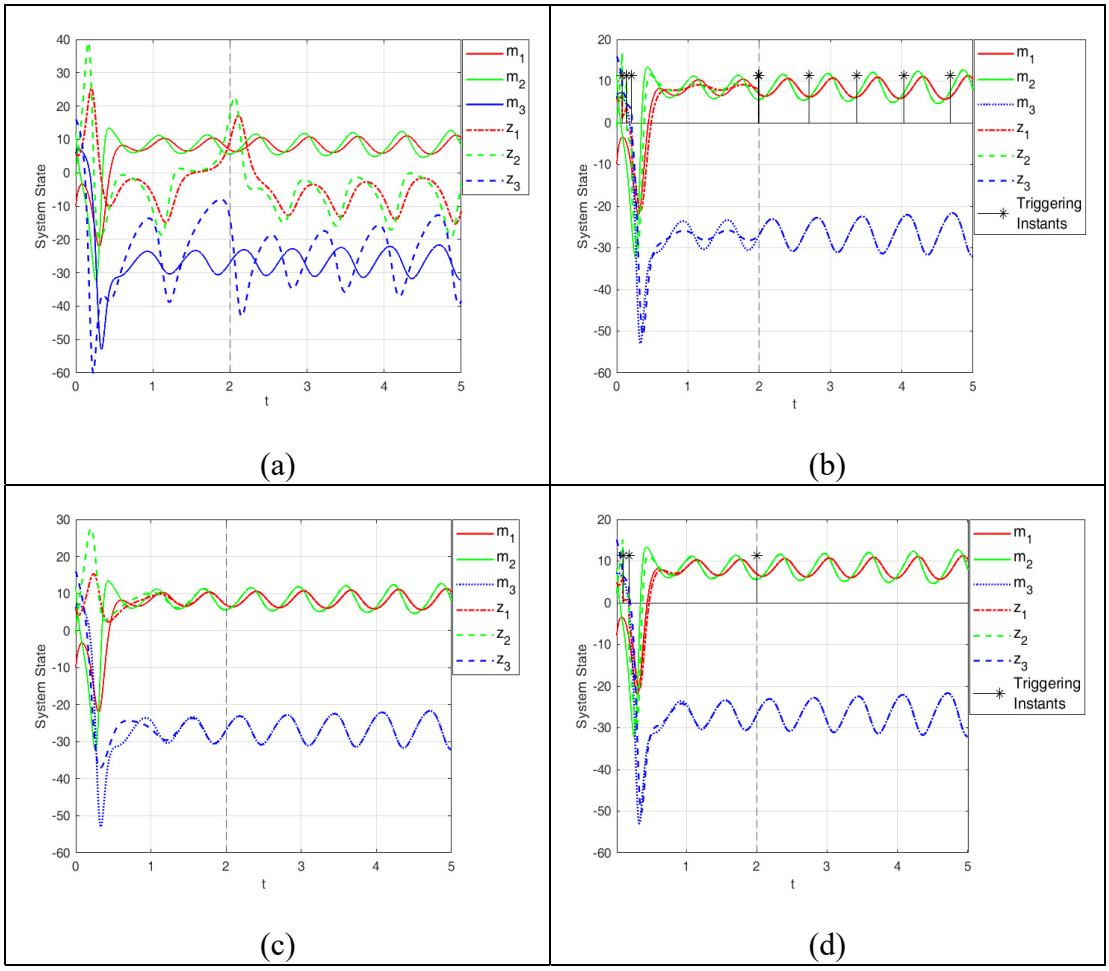

Figure 2. 2D trajectories of system (34): (a) No control; (b) DETIC only; (c) Continuous control only; (d) Hybrid control.

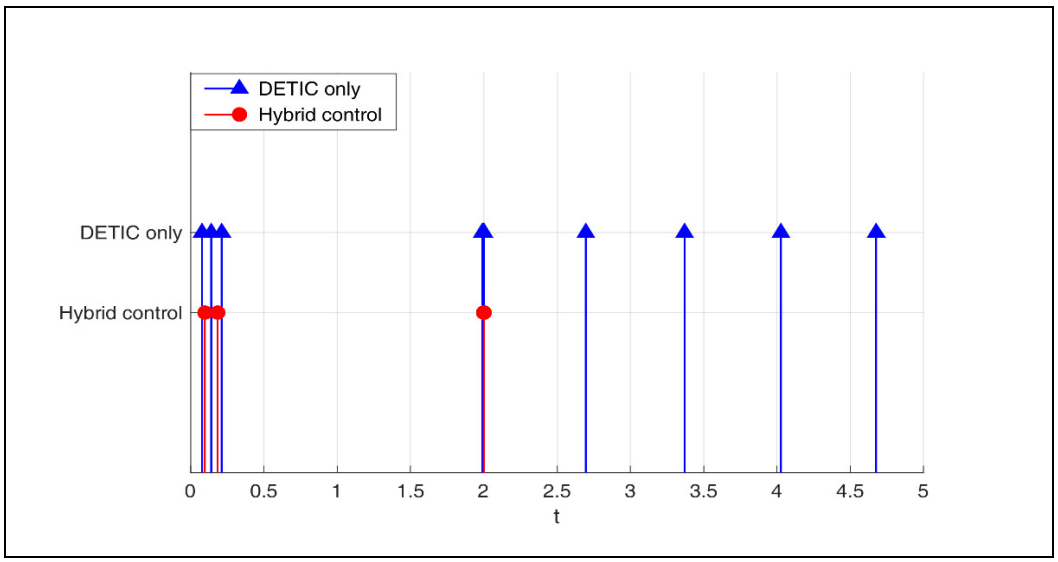

Figure 3. Triggering instants of DETIC only and hybrid control.

Figure 4 shows the trajectories of the error system (24) for system (34) with the above four cases. It is illustrated that only DETIC can achieve the sudden drop of error, but the oscillation is large. Only continuous control can achieve a smooth convergence, but the speed is relatively slow. Hybrid control maintains a higher steady-state accuracy. Specifically, hybrid control achieves a convergence time of 1.567 seconds, which is 21.3% faster than that of only DETIC (1.992 seconds). Moreover, at 1.0 second, the error of hybrid control is 0.4881 and represents a 77.1% reduction compared to that of only DETIC (2.1273 seconds), thus revealing the superiority of hybrid control.

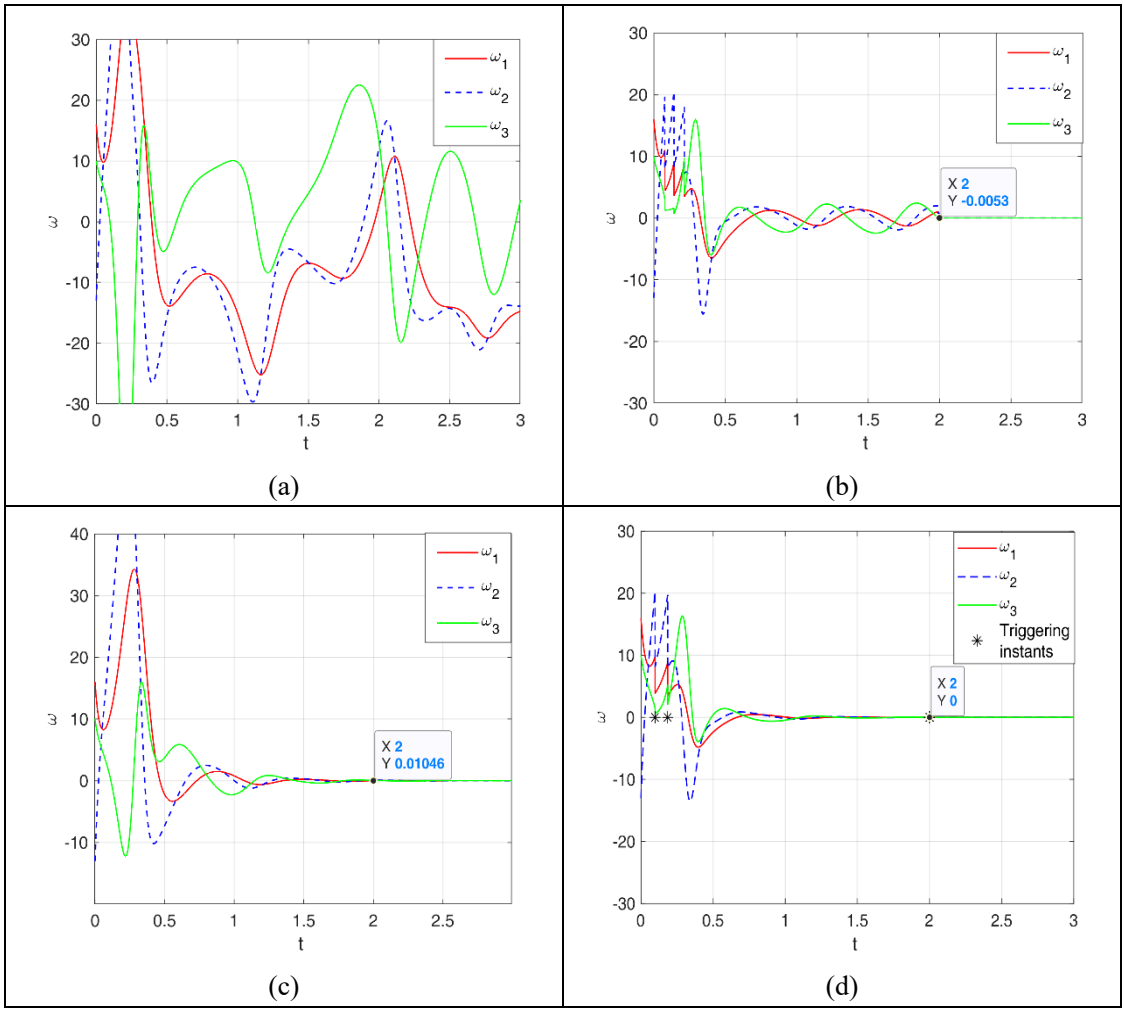

Figure 4. Trajectories of error system (24) for system (34): (a) No control; (b) DETIC only; (c) Continuous control only; (d) Hybrid control.

Figure 5 shows energy evolutions of the error system (24) for system (34) under logarithmic coordinates for the above four cases. Under only continuous control, the error shows a slow decreasing trend, thus exhibiting slow convergence. Under only DETIC, the error significantly decreases at each triggering instant and converges faster than that under only continuous control. The hybrid control not only reduces the error energy quickly when the error is large, but also maintains its stability through continuous control on the triggering intervals, thus achieving the best performance. Here, all control strategies ultimately achieve a zero steady-state error, but the hybrid control accomplishes this with 47.8% fewer triggering numbers, thus highlighting its advantage in the control efficiency.

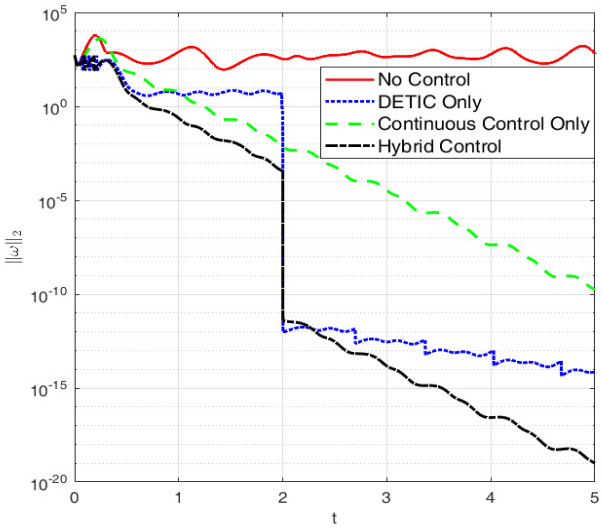

Figure 5. Logarithmic-scale error energy evolution of error system (24) for system (34).

In conclusion, the hybrid control strategy achieves a comprehensive improvement in the control efficiency, dynamic performance, convergence speed, and other aspects while maintaining a good synchronization accuracy, and has significant superiority in the control of complex systems.

6. Conclusions

A DETIC strategy, coordinated with continuous control, was designed to resolve the PTS problem in nonlinear systems. Furthermore, the method was extended to the master-slave synchronization problem and validated through simulations of chaotic Lorenz system. Although our DETM showed significantly improvements over the traditional method and performed well in adapting to system state changes and ensuring the stability of the specified time, there remains room for further optimization.

Future work will focus on the design of a self-triggered impulsive control strategy. Specifically, we will construct an analytical function, from the perspectives of system's Lyapunov function and prescribed-time stability requirements, to directly compute the next triggering interval. This approach is designed to fundamentally eliminate the need for continuous state monitoring, thereby resolving the persistent monitoring overhead inherent in current dynamic event-triggered mechanisms. Moreover, we plan to verify the superiority of this self-triggering mechanism in the control performance and resource efficiency in complex environments with more demanding communication resources (such as bandwidth limitations and packet loss) or unknown disturbances.

Use of AI tools declaration

The authors declare they have not used Artificial Intelligence (AI) tools in the creation of this article.

Acknowledgments

This project is jointly supported by the Humanities and Social Science Fund of Ministry of Education of China (23YJAZH031), the Natural Science Foundation of Hebei Province of China (A2023209002,

A2019209005), the Tangshan Science and Technology Bureau Program of Hebei Province of China (24130201C) and Fundamental Research Funds for Hebei Province Universities: North China University of Science and Technology (No. JJC2024045).

Conflict of interest

The authors declare there is no conflict of interest.

Author contributions

Yanmei Yang: Investigation, Validation, Funding acquisition, Writing; Xiaoying Zhu: Investigation, Methodology, Writing, Validation; Lichao Feng: Conceptualization, Investigation, Supervision, Writing; Liping Du: Writing and Software.

References

1. J. Hahn, M. Mönnigmann, W. Marquardt, A method for robustness analysis of controlled nonlinear systems, *Chem. Eng. Sci.,* **59** (2004), 4325–4338. https://doi.org/10.1016/j.ces.2004.06.026
2. Z. H. Zhao, T. Wang, J. Y. Yu, M. V. Basin, Bilateral cooperative control of nonlinear multiagent systems with state and output quantification, *IEEE Trans. Cybern*., **55** (2025), 2949–2957. https://doi.org/10.1109/TCYB.2025.3545144
3. Z. H. Zhao, J. Y. Yu, T. Wang, F. Peng, Adaptive fuzzy resilient decentralized control for nonlinear large-scale CPSs under DoS attacks, *IEEE Trans. Fuzzy Syst.*, **32** (2024), 5899–5909. https://doi.org/10.1109/TFUZZ.2024.3434726
4. S. J. Fan, T. Wang, C. H. Qin, J. B. Qiu, M. Li, Optimized backstepping attitude containment control for multiple spacecrafts, *IEEE Trans. Fuzzy Syst*, **32** (2024), 5248–5258. https://doi.org/10.1109/TFUZZ.2024.3418577
5. T. Yang, Practical stability of impulsive control, in *Impulsive Control Theory*, Springer, Berlin, Heidelberg, (2001), 149–197. https://doi.org/10.1007/3-540-47710-1_6
6. E. G. Gilbert**,** G. A. Harasty, A class of fixed-time fuel-optimal impulsive control problems and an efficient algorithm for their solution, *IEEE Trans. Autom. Control*, **16** (1971), 1–11. https://doi.org/10.1109/TAC.1971.1099656
7. X. Z. Liu, K. X. Zhang, Input-to-state stability of time-delay systems with delay-dependent impulses, *IEEE Trans. Autom. Control*, **65** (2019), 1676–1682. https://doi.org/10.1109/TAC.2019.2930239
8. W. L. He, X. Y. Gao, W. M. Zhong, F. Qian, Secure impulsive synchronization control of multi-agent systems under deception attacks, *Inf. Sci.*, **459** (2018), 354–368. https://doi.org/10.1016/j.ins.2018.04.020
9. X. Y. He, X. D. Li, S. J. Song, Prescribed-time stabilization of nonlinear systems via impulsive regulation, *IEEE Trans. Syst., Man, Cybern*., **53** (2022), 981–985. https://doi.org/10.1109/TSMC.2022.3188874
10. A. Anta, P. Tabuada, To sample or not to sample: Self-triggered control for nonlinear systems, *IEEE Trans. Autom. Control*, **55** (2010), 2030–2042. https://doi.org/10.1109/TAC.2010.2042980

11. H. Shen, C. J. Peng, H. C. Yan, S. Y. Xu, Data-driven near optimization for fast sampling singularly perturbed systems, *IEEE Trans. Autom. Control*, **69** (2024), 4689–4694. https://doi.org/10.1109/TAC.2024.3352703
12. D. P. Yang, W. Ren, X. D. Liu, W. S. Chen, Decentralized event-triggered consensus for linear multi-agent systems under general directed graphs, *Automatica,* **69** (2016), 242–249. https://doi.org/10.1016/j.automatica.2016.03.003
13. M. Abdelrahim, R. Postoyan, J. Daafouz, D. Nešić, Robust event-triggered output feedback controllers for nonlinear systems, *Automatica*, **75** (2017), 96–108. https://doi.org/10.1016/j.automatica.2016.09.044
14. H. Shen, W. Zhao, J. D. Cao, J. H. Park, J. Wang, Predefined-time event-triggered tracking control for nonlinear servo systems: A fuzzy weight-based reinforcement learning scheme, *IEEE Trans. Fuzzy Syst.*, **32** (2024), 4557–4569. https://doi.org/10.1109/TFUZZ.2024.3403917
15. Z. H. Zhang, G. H. Yang, Event-triggered fault detection for a class of discrete-time linear systems using interval observers, *ISA Trans.*, **68** (2017), 160–169. https://doi.org/10.1016/j.isatra.2016.11.016
16. X. Y. Meng, L. H. Xie, Y. C. Soh, Asynchronous periodic event-triggered consensus for multi-agent systems, *Automatica*, **84** (2017), 214–220. https://doi.org/10.1016/j.automatica.2017.07.008
17. Y. P. Guan, Q. L. Han, X. H. Ge, On asynchronous event-triggered control of decentralized networked systems, *Inf. Sci.*, **425** (2018), 127–139. https://doi.org/10.1016/j.ins.2017.10.024
18. X. D. Li, D. G. Peng, J. D. Cao, Lyapunov stability for impulsive systems via event-triggered impulsive control, *IEEE Trans. Autom. Control*, **65** (2020), 4908–4913. https://doi.org/10.1109/TAC.2020.2964558
19. H. L. Liu, T. X. Zhang, X. D. Li, Event-triggered control for nonlinear systems with impulse effects, *Chaos Solitons Fractals*, **153** (2021), 111499. https://doi.org/10.1016/j.chaos.2021.111499
20. X. D. Li, P. Li, Input-to-state stability of nonlinear systems: Event-triggered impulsive control, *IEEE Trans. Autom. Control*, **67** (2021), 1460–1465. https://doi.org/10.1109/TAC.2021.3063227
21. L. C. Feng, M. Y. Dai, N. Ji, Y. L. Zhang, L. P. Du, Prescribed-time stabilization of nonlinear systems with uncertainties/disturbances by improved time-varying feedback control, *AIMS Math.*, **9** (2024), 23859–23877. https://doi.org/10.3934/math.20241159
22. W. L. Lu, X. W. Liu, T. P. Chen, A note on finite-time and fixed-time stability, *Neural Networks*, **81** (2016), 11–15. https://doi.org/10.1016/j.neunet.2016.04.011
23. H. Shen, X. Yu, H. C. Yan, J. H. Park, J. Wang, Robust fixed-time sliding mode attitude control for a 2-DOF helicopter subject to input saturation and prescribed performance, *IEEE Trans. Transp. Electrif.*, **11** (2024), 1223–1233. https://doi.org/10.1109/TTE.2024.3402316
24. K. X. Zhang, B. Gharesifard, Hybrid event-triggered and impulsive control for time-delay systems, *Nonlinear Anal. Hybrid Syst.*, **43** (2021), 101–109. https://doi.org/10.1016/j.nahs.2021.101109
25. T. H. Yu, Y. Z. Liu, J. D. Cao, Finite-time stability of dynamical system under event-triggered hybrid control, *Appl. Math. Model.*, **117** (2023), 286–295. https://doi.org/10.1016/j.apm.2022.12.031
26. J. L. Liu, Y. D. Wang, J. D. Cao, D. Yue, X. P. Xie, Secure adaptive-event-triggered filter design with input constraint and hybrid cyber attack, *IEEE Trans. Cybern.*, **51** (2020), 4000–4010. https://doi.org/10.1109/TCYB.2020.3003752

27. W. L. He, B. Xu, Q. L. Han, F. Qian, Adaptive consensus control of linear multiagent systems with dynamic event-triggered strategies, *IEEE Trans. Cybern.*, **50** (2019), 2996–3008. https://doi.org/10.1109/TCYB.2019.2920093
28. Q. Li, B. Shen, Z. D. Wang, T. W. Huang, J. Luo, Synchronization control for a class of discrete time-delay complex dynamical networks: A dynamic event-triggered approach, *IEEE Trans. Cybern.*, **49** (2018), 1979–1986. https://doi.org/10.1109/TCYB.2018.2818941
29. X. N. Li, H. Q. Wu, J. D. Cao, Prescribed-time synchronization in networks of piecewise smooth systems via a nonlinear dynamic event-triggered control strategy, *Math. Comput. Simul.*, **203** (2023), 647–668. https://doi.org/10.1016/j.matcom.2022.07.010
30. X. N. Li, H. Q. Wu, J. D. Cao, A new prescribed-time stability theorem for impulsive piecewise-smooth systems and its application to synchronization in networks, *Appl. Math. Model.*, **115** (2023), 385–397. https://doi.org/10.1016/j.apm.2022.10.051
31. C. C. Li, C. Y. Zhang, L. C. Feng, Z. H. Wu, Note on prescribed-time stability of impulsive piecewise-smooth differential systems and application in networks, *Networks Heterog. Media*, **19** (2024), 970–991. https://doi.org/10.3934/nhm.2024043
32. L. C. Feng, C. C. Li, Abdel-Aty. Mahmoud, J. D. Cao, Prescribed-time stability of nonlinear impulsive piecewise systems and synchronization for dynamical networks, *Qual. Theory Dyn. Syst.*, **24** (2025), 165. https://doi.org/10.1007/s12346-025-01302-1

AIMS Press